Egyptian Journal of Chemistry

http://ejchem.journals.ekb.eg/

QTAIM VIEW OF Os–Os BONDING IN TRIOSMIUM CLUSTERS [Os_3 (CO) $_9$(μ-η^2-C_7H_3 (2-CH_3) NS) (μ-CH_2) CH_3]

Muhsen Abood Muhsen Al-Ibadi[1*], Nadia Ezzat Al-kirbasee[2], Shatha Raheem Helal Alhimidi[3], Baker A. Joda[4], Manal A. Mohammed[5]

[1] *Department of Chemistry, College of Science, University of Kufa, Iraq*
[2] *Department of Chemistry, College of Education for Women, University of Kufa, Iraq*
[3] *Department of Basic Medical Science, College of Dentistry, Al-Muthanna University, Iraq*
[4]*Department of Chemistry, College of Science, University of Kerbala, Iraq*
[5] *Department of Basic Science, College of Dentistry, University of Kerbala, Iraq*

Abstract

The topological features of the Triosmium cluster [$Os_3(CO)_9(\mu$-η^2-$C_7H_3(2$-$CH_3)NS)(\mu$-$CH_2)CH_3$], containing carbonyl and 2-methylbenzothiazol ide ligands, has been examined using density functional theory (DFT) and QTAIM-based "Quantum Theory Atoms in Molecules". The topological parameters of the electron density in the cluster have been calculated. The QTAIM analysis of the topological features demonstrated that the core part Os_3C1 in the cluster is significantly absence a bond critical point and its bond path between Os_1-Os_3. Whereas, the analysis Os_1-Os_2 and Os_2-Os_3 interactions revealed the occurrence of bond paths and bond critical points between these atoms. A multicentre 4c–5e interaction for the Os_3C1 core has been proposed. The topological parameters calculation show that the interactions in the bridging 2-methylbenzothiazolide Ligand are a typical for shared shell with the existence of some double-bond character.

Keywords:- DFT calculations, QTAIM, Metal–metal bonds, Organometallic complexes, Topological analysis.

Introduction

Electron-deficient benzoheterocyclic triosmium clusters has been of special interest in the area of recent organometallic chemistry[1].The structures and reactivity of electron-deficient compound and their product are very sensitive on the nature of the substituent group of the heterocyclic ring[2-5]. Chemistry of electron-deficient triosmium clusters has been widely studied in recent years because of their high reactive comparative to their electron precise counterparts[2,6,7]. Quantum theory of atoms in molecules(QTAIM) are an important methodology to describe the bonding in the organometallic system[8]. The core of this methodology is defining and characterizing a chemical bond through bond critical point (bcp) along of an atomic interaction line in an equilibrium geometry(bond bath)[9-11]. At this bond critical point, computing the topological parameters, such as electron density (ρ_b), the Laplacian ($\nabla^2\rho b$) and the electronic energy density (H_b) give us a useful information about the bonding situation in chemical compounds[12-16]. The aim of our study is to exploring of the M–M and M–ligand interactions properties in "[$Os_3(CO)_9(\mu$-η^2-$C_7H_3(2$-$CH_3)NS)(\mu$-$CH_2)CH_3$]"[17] as shown in Figure 1. Our results might be important due to an interesting comparisons between the different topological features of the

* **Muhsen Abood Muhsen Al-Ibadi** e-mail: *muhsen.alibadi@uokufa.edu.iq ; (*University of Kufa, Iraq*).
Receive Date: 28 March 2020, Revise Date: 06 June 2020, Accept Date: 15 July 2020
DOI: 10.21608/EJCHEM.2020.26737.2546

interaction between Os-Os metals, the influence of bridging ligand (μ^2-CH_2 and 2-methylbenzothiazolide) in the Os-Os interactions, and comparison several topological properties with the other interaction such Os–N and Os-C bonds in the cluster. Additionally, the interactions in the bridging 2-methylbenzothiazolide ligand were discussed in detail.

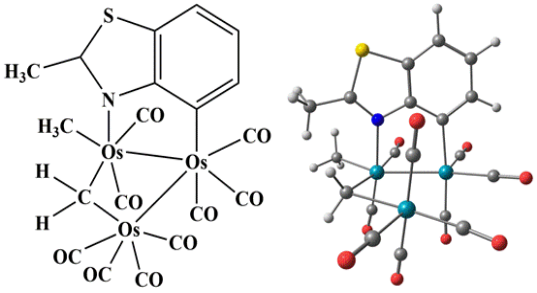

Figure 1: (a) molecular structure and (b) geometry optimization of "[$Os_3(CO)_9(\mu$-η^2-$C_7H_3(2$-$CH_3)NS)(\mu$-$CH_2)CH_3$]"

Theoretical Methods

The structure of Triosmium cluster in the gas phase was fully optimized using Density functional theory (DFT). Frequency calculations confirmed it as minima on the potential energy surface. By using Gaussian 09 program[18], a PBE1PBE[19] functional was used, associated with all-electron 6-31G(d,p) for C, H, N,,S and O atoms and SDD[20] effective core potential (ECP) for Os basis sets. The topological parameters were computed, at PBE1PBE /WTBS[23] for Os /6-31G (d, P)[21] for other atoms, using AIM2000 program package[22].

Results and Discussion

. The geometry structure of triosmium cluster species under study is optimized and a representative structure is shown in Figure 1-b. Using AIM program, the molecular graph of the cluster is illustrated in Figure 2, where addressed a bond paths and bond and ring critical points. Inspection on this molecular graph finds that: (i) The bond critical point with its bond path between Os_1-Os_3 is not found which is an indicator of absence a chemical bond (ii) The bond paths with a bond critical points corresponding to Os_1-Os_2 and Os_2-Os_3 bonds are exist. (iii) A set of bond paths and bond critical points within Os-C, C-O, C-S, C-N and C-C bonds and four ring critical points related Os_1-Os_2-Os_3-C_1, Os_2-C_3-C_8-N_1-Os_3, C_3-C_4-C_5-C_6-C_7-C_8, C_7-C_8-N_1-C_9-S_1 rings were found.

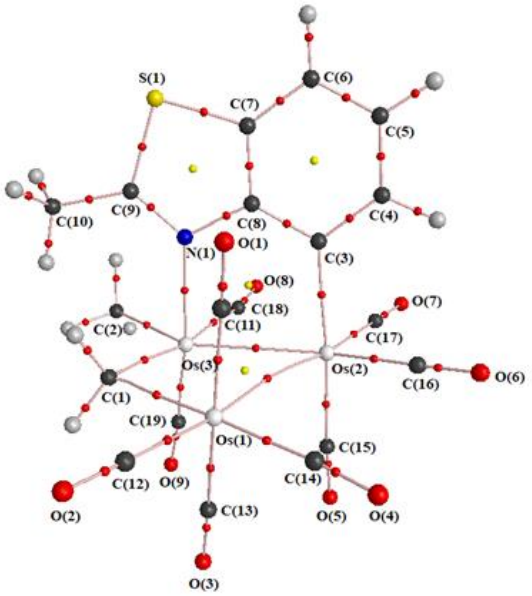

Figure 2. The molecular graph and the bond and ring critical points, which are shown as red and yellow circles, respectively, for the cluster.

Gradient trajectory maps of the triosmium core plane Os_1-Os_2-Os_3-C_1 are plotted in Figure 3. Inspecting the Os_1-Os_2 and Os_2-Os_3 bonds reveals the existence bond paths, bond critical points, and atomic basins. Differently, no bond critical point or bond path is observed for Os_1-Os_3. Additionally, in the plot, one bridged Carbon C_1 with bond critical points and bond baths are visible.

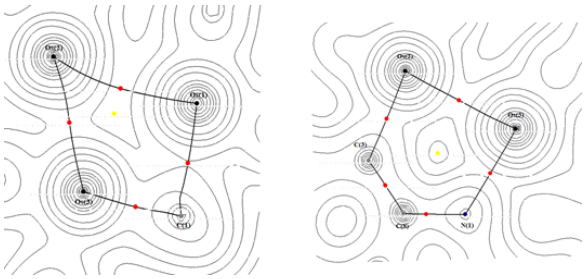

Figure 3: Gradient trajectories map in the plane through (a) Os_1- Os_2- Os_3-C_1 (b) Os_2-C_3-C_8-N_1-Os_3 in complex.

Additionally, the map of 2-methylbenzothiazolide ligand display a six-membered cyclic with one ring critical point and five-membered ring having one ring critical point and one C−C, two N−C, and two S-C bond critical points as seen in Figure 4. Also, in this figure, the bond paths and bond critical points between the interaction of Os_3 and Os_2 with N_1 and C_3 respectively, are observed.

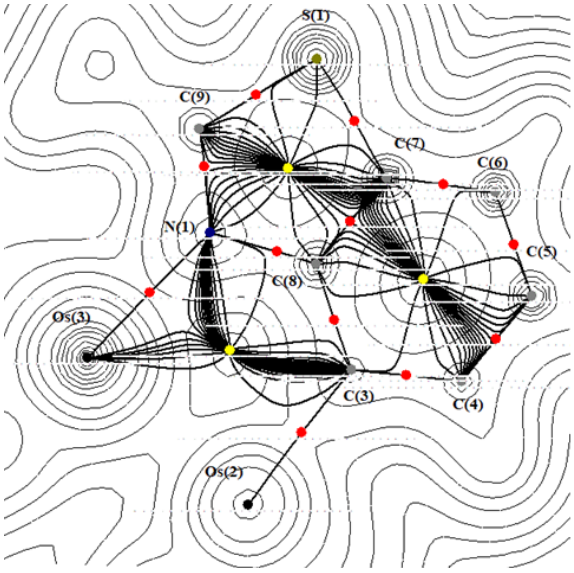

Figure 4: Gradient trajectories map in the plane through 2-methylbenzothiazolide ligand in complex.

Within the conceptual framework of the QTAIM Theory, the Laplacian ($\nabla^2\rho_b$) is an indicator for classification of the interactions between atoms in two types: shared (covalent bond) and closed-shell interactions (ionic bond). For the former interactions, the electronic charge is concentrated towards the line of interaction running between two nuclei ($\nabla^2\rho_b < 0$), whereas for later interactions electronic charge is depleted toward each of the interacting nuclei ($\nabla^2\rho_b > 0$). On the other hand, the total electronic energy densities(H_b) at bond critical points will be a more appropriate index for interactions[23,24], where $\mathbf{H_b = G_b + V_b}$ [G_b kinetic energy densities and ($V(r_b)$) the potential energy] dewhere[25-27]. Consequently, $H_b < 0$ with$\nabla^2\rho r_b < 0$ for covalent bonds ,$H_b > 0$ with $\nabla^2\rho_b > 0$ for ionic bonds and Hr < 0 with $\nabla^2\rho_b > 0$ for transit-closed interaction[28-30].
The calculated of local properties of electron density at the bond critical points for the triosmium cluster are given in Table 1.

For the core part Os3C(1), as seen from Table 1, the BCP Laplacian of the Os_1-$Os_2$and Os_2-Os_3 bonds are small positive values (0.037and0.093, respectively). Additionally, the small BCP electron density values (0.032 and 0.049, respectively) with the small negative values of H_b (-0.004 and-0.009, respectively) are corresponding to a metal-metal open-shell interaction. Comparison of the BCP electron density and its laplacian for Os_1-Os_2 and Os_2-Os_3 bonds with the electron density and laplacian at the unbridged Os-Os bonds for the compounds "$[Os_3(CO)_{12}]$, $[Os_3(\mu\text{-}H)_2(CO)_{10}]$, $[Os_3(\mu\text{-}H)(\mu\text{-}OH)(CO)_{10}]$, and $[Os_3(\mu\text{-}H)(\mu\text{-}Cl)(CO)_{10}]$"[31]. Showed that the strong interaction between Os_1 and Os_2 metal atoms with 2-methylbenzothiazolide ligand led to lowering the electron density and the laplacian values (positive values) and then lowering of the covalent contribution to both Os_1-$Os_2$and Os_2-Os_3 bonds. Regarding to the bridged Os_1 and Os_3 atoms, a key point is the nonexistence of a bond path with its bond critical point. Thus pointing out that there is no_localized electron concentration between these two Osmium atoms led to conclude that the strong interactions of bridging C ligand destroy the topological Os_1- Os_3 bond.

From the literature, the bond critical points with its bond path have been found between unsupported M-M bond, for example Co-Co and Mn-Mn in "$Co_2(CO)_6(Asph_3)_2$"[32] and $Mn_2(CO)_{10}$[33] respectively. Conversely, a bond path and bond critical point have also been found for the interaction a transition metal with strong bridging ligand, for instance, Mo-Mo in "$[Mo_3(\mu^2\text{-}S)_3(\mu^2\text{-}S)Cl_3(PH_3)_6]^+$"[34]. The laplacian map for the core $Os_3C(1)$, as seen in Figure5, show the VSCCs of bridging carbon are obviously shifted across a midpoint of the Os-Os interaction.

We also calculated the delocalization indices for the interactions in the Os3C (1) core, Table 2. The calculated delocalization indices values for the Os_1-Os_2 and Os_2-Os_3 bonds (0.328 and 0.471, respectively) are comparable to the Ru-Ru bond (0.458 on average) in "$[Ru_3(\mu\text{-}H)_2(\mu^3\text{-}MeImCH)(CO)_9]$"[35]. Os-Os bonds (wthin the range 0.350 -0.461) in "$[Os_3(CO)_{12}]$, $[Os_3(\mu\text{-}H)(\mu\text{-}C_l)(CO)_{10}]$, $[Os_3(\mu\text{-}H)(\mu\text{-}OH)(CO)_{10}]$ and $[Os_3(\mu\text{-}H)_2(CO)10]$"[31] and Fe-Fe bond (0.398 on average) in $[Fe_3(\mu\text{-}H)(\mu\text{-}COMe)(CO)_{10}]$[36]. Furthermore, the obtained values are correlated with computed values for other M-M interactions[37]. By reasons of nonbonding interaction, small $Os_1 \ldots Os_3$ delocalization indices was obtained (0.277) Table 2. This calculated value was consistent with the hydride-bridged metal...metal non-bonding interactions Ru...Ru (within range 0.169-0.246) in "$[Ru_3(\mu\text{-}H)_2(\mu^3\text{-}MeImCH)(CO)_9]$"[35], Os...Os (0.177) in $[Os_3(\mu\text{-}H)(\mu\text{-}Cl)(CO)_{10}]$[31], and Fe...Fe (0.208) in $Fe_3(\mu\text{-}H)(\mu\text{-}COMe)(CO)_{10}]$[38] and compare well to those found for other organometallic compounds[38,39,40]. From other side, the nonbonding $Os_1 \ldots Os_3$ delocalization indices is correlated to other studies reported for unbridged M-M interaction ex. Co-Co interaction in $[Co_2(CO)_8]$ (0.460)[41]. As the bridged $Os_1 \ldots Os_3$ interaction, the delocalization index value is smaller than that of unbridged Os-Os interaction. Regarding to Os-C_1 bonds, the topological properties will discussed in next section. When we sum up the delocalization indexes δ(A–B) for bonding and nonbonding interactions in the core, shown in Table. 3, are equal to the value of 2.581. Therefore, the interaction

in the core part Os3C(1) of the cluster is essentially explained by 4c–5e.

Table 1. The local properties of electron density at critical points of the bonds of Cluster.

Bond	ρr_b(eÅ)	$\nabla^2\rho r_b$(eÅ)	Gr_b(he)	Hr_b(he)	Vr_b(he)	εr_b
Os_1-Os_2	0.032	0.037	0.013	-0.004	-0.018	0.652
Os_2-Os_3	0.049	0.093	0.032	-0.009	-0.042	0.039
Os_1-C_1	0.079	0.132	0.055	-0.022	-0.077	0.105
Os_3-C_1	0.129	0.243	0.113	-0.052	-0.165	0.037
Os-$C_{(CO)}$*	0.148	0.483	0.184	-0.063	-0.247	0.055
Os_2-C_3	0.108	0.209	0.089	-0.037	-0.126	0.042
Os_3-N_1	0.074	0.361	0.099	-0.008	-0.108	0.085
N_1-C_8	0.293	-0.796	0.190	-0.389	-0.579	0.108
N_1-C_9	0.353	-0.889	0.308	-0.531	-0.839	0.231
S_1-C_7	0.208	-0.397	0.063	-0.162	-0.226	0.187
S_1-C_9	0.210	-0.404	0.067	-0.168	-0.236	0.261
C_9-C_{10}	0.255	-0.618	0.067	-0.222	-0.289	0.037
C-O*	0.460	0.521	0.930	-0.8	-1.731	0.002

*** Average**

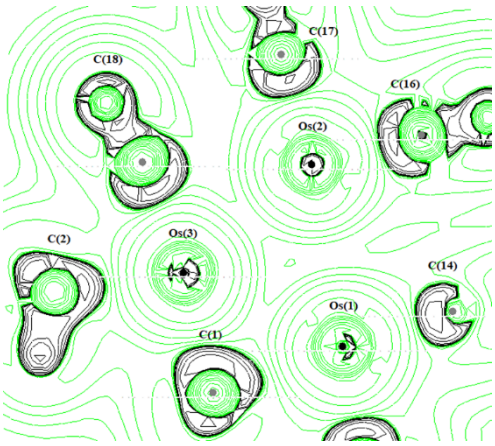

Figure 5. shows the plots of the Laplacian distribution in the core(Os3C(1)) plane

Table 2. Delocalization indexes for selected interactions.

Atom (A, B)	δ(A, B)
Os_1-Os_2	0.328
Os_1…Os_3	0.277
Os_2-Os_3	0.471
Os_1-C_1	0.599
Os_2-C_1	0.029
Os_3-C_1	0.877
Os_1-N_1	0.012
Os_2-N_1	0.015
Os_3-N_1	0.418

For Os-C$_1$ bonds, given in Tables 1, the computed BCP electron density, Laplacian and electronic energy density H properties for both Os–C_1 bonds showed that both bonding have lower ρ_b (0.079 and 0.129 Å^{-5}), positive $\nabla^2\rho_b$ (0.132 and 0.243 Å^{-5}) and negative H_b (-0.022 and -0.052he^{-1}) values which is typical for open-shell coordination bonding. The results obtained were in line with the computed data for bridging ligands such as CO, H and CH[35,42,43,44]. In comparison with the Os-C(co) bonds, the BCP topological values of Os-C(co) bonds are higher than the Os-C_1 bonds might be explained by their higher polarity of CO group. Regarding to the bonds between Os atoms with the 2-methylbenzothiazolide ligand the BCP Laplacians of both Os–C_3 and Os-N_1 bonds are positive (0.209 and 0.361 Å^{-5}), with low ρ_b values (0.108 and 0.074 Å^{-5}) and a negative H_b values for (-0.037 and -0.008 he^{-1}) as expected, for open-shell interactions. Figure 2 and Figure 4 depict the molecular graph and the gradient trajectory map, respectively, of the bridging 2-methylbenzothiazolide ligand in the cluster. As expected for polar bonds, excepting C-C bonds, the BCPs are arranged in the middle of the bond path, the BCPs on the C-N and C-S bonds are displaced to the less electronegative atom. The BCP characteristics of the bonding interaction within the bridging 2-methylbenzothiazolide ligand atoms are listed in Tables 1. The BCP Laplacians of all bonds within the bridging 2-methylbenzothiazolide ligand are negative as expected, for sharing coordination bonding (covalent bonds). Interestingly, The BCP ellipticity values of C-S bonds are higher than C-N indicate that the C-S bonds have a π-character more than C-N bonds.

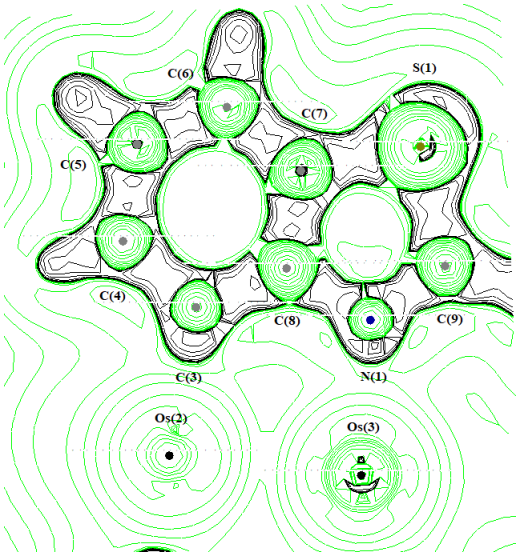

Figure 6. Shows the plots of the Laplacian distribution of the Os$_2$-Os$_3$-N$_1$ plane

The nature of the interactions of the 2-methylbenzothiazolide ligand bonds are shown in the map of the Laplacian (Figure 7). The electron cloud in the VSCCs of C_3 atom is polarised to the Os_2, whereas the N_1 atom polarised to the Os_3.

Conclusion

A topological properties of the electron density distribution for triosmium cluster [$Os_3(CO)_9(\mu\text{-}\eta^2\text{-}C_7H_3(2\text{-}CH_3)NS)(\mu\text{-}CH_2)CH_3$] have been calculated and interpreted by QTAIM theory. The topological properties of the bonding interaction was analyzed and compared with the previous studies. The QTAIM analyses of the Os3C(1) core part reveal, on one hand, existence the bond paths and bond critical points in the Os_1-Os_2 and Os_2-Os_3 interactions. On the other hand, neither bond path nor bond critical point between Os_1-Os_3 interaction is observed, although for these non-bonding interactions, a non-negligible delocalization index has been computed. Consequently, the interaction in the core part can be described as multiple 4c–5e bonding interaction. Inspection of the topological features of the bonding interactions in the bridging 2-methylbenzothiazolide ligand finds that all these bonds are typical for shared shell with the presence of some double-bond character.

Acknowledgement
We gratefully acknowledge the funding from department of chemistry in university of Kufa.

Reference

1. Begum, S. A., Chowdhury, A.H., Ghosh, S. & Tocher, D.A.. *Inorganica Chim. Acta* **478**, 25–31 (2018).
2. Ghosh, S., Uddin, M.N., Begum, N. & Hossain, G.M.G.. *J. Chem. Crystallogr.* **40**, 572–578 (2010).
3. Hossain, M. I., Ghosh, S., Hogarth, G., Golzar Hossain, G. M. & Kabir, S. E. *J. Organomet. Chem.* **696**, 3036–3039 (2011).
4. Din, A. B., Bergman, B., Rosenberg, E., Smith, R. & Gobetto ,R. *Polyhedron* **17**, 2975–2984 (1998).
5. Kabir, S. E., Kolwaite, D.S. & Rosenberg, E. *Organometallics* **14**, 3611–3613 (1995).
6. Deeming, A. J. *in Advances in organometallic chemistry*, **26**, 1–96 (1986).
7. Suss-Fink, G. & Meister, G. *in Advances in organometallic chemistry* **35**, 41–134 (1993).
8. Nakanishi, W., Hayashi, S. & Narahara, K. *J. Phys. Chem. A* **112**, 13593–13599 (2008).
9. Gatti, C. Cryst. *Mater.* **220**, 399 **(2005)**.
10. Kovacs, A., Kolossvary, I., Csonka, G. I. & Hargittai, *J. Comput. Chem.* **17**, 1804–1819

(2005).
11. Grimme, S. *J. Am. Chem. Soc.* **118**, 1529–1534 (1996).
12. Gatti, C. & Lasi, D. *Organometallic Compounds*. 55–78 (2007).
13. Bader, R. F. W. *Chem. Rev*., **91**, 893, (1991).
14. Volkov, A., Abramov, Y. & Gatti, C. *Acta Cryst. A* 332–339 (2000).
15. Koritsanszky, T. S. & Coppens, P. Chemical applications of X-ray charge-density analysis. *Chem. Rev.* **101**, 1583–627 (2001).
16. Alhimidi, S. R. H., Al-Ibadi, M. A. M., Hasan, A. H. & Taha, A. *Journal of Physics: Conference Series* **1032**, 12068 (2018).
17. Kabir, S. E., Malik, K.M.A., Mandal, H.S. & Mottalib M.A. *Organometallics* **21**, 2593–2595 (2002).
18. Gaussian09, R. 01, Frisch MJ et al., Gaussian. *Inc., Wallingford CT* (2009).
19. Adamo, C. & Barone, V. *J. Chem. Phys.* **110**, 6158–6170 (1999).
20. Fuentealba, P., Preuss, H., Stoll, H. & Von Szentpály, L. *Chem. Phys. Lett.* **89**, 418–422 (1982).
21. Hehre, W. J., Ditchfield, R. & Pople, J. A. *J. Chem. Phys.* **56**, 2257–2261 (1972).
22. Bader, R. F. W., Biegler-König, F. & Schönbohm, J. AIM2000 program package. (2002).
23. Theivarasu, C. & Murugesan, R. *Int. J. Chem. Sci.* **14**, 67–87 (2016).
24. Cremer, D. & Kraka, E. *Angew. Chemie Int. Ed. English* **23**, 627–628 (1984).
25. Bianchi, R., Gervasio, G. & Marabello, D. *Comptes Rendus Chim.* **8**, 1392–1399 (2005).
26. Khan, S. A., Shahid, S., Kanwal, S. & Hussain, G. *Dye. Pigment.* **148**, 31–43 (2018).
27. Kumar, P. S. V., Raghavendra, V. & Subramanian, V. Bader's. *J. Chem. Sci.* **128**, 1527–1536 (2016).
28. CVan Der Maelen, Juan F.abeza, J. A. *Inorganic Chemistry* **51**, 7384–7391 (2012).
29. Bobrov, M. F., Popova, G. V. & Tsirelson, V. G. A *Russ. J. Phys. Chem.* **80**, 584–590 (2006).
30. Goli, M. & Shahbazian, S. *Theoretical Chemistry Accounts,***129**, 235-245, (2011).
31. Van der Maelen, J. F., García-Granda, S. & Cabeza, *J. A. Comput. Theor. Chem.* **968**, 55–63 (2011).
32. Macchi, P., Proserpio, D. M. & Sironi, A. *J. Am. Chem. Soc.* **120**, 13429–13435 (1998).
33. Farrugia, L. J., Mallinson, P. R. & Stewart, B. *Acta Crystallogr. Sect. B Struct. Sci.* **59**, 234–247 (2003).
34. Feliz, M., Llusar, R., Andrés, J., Berski, S. & Silvi, B. *New J. Chem.* **26**, 844–850 (2002).
35. Cabeza, J. A., Van der Maelen, J. F. & García-Granda, S. *Organometallics* **28**, 3666–3672 (2009).
36. Farrugia, L. J. & Senn, H. M. *J. Phys. Chem. A* **114**, 13418–13433 (2010).
37. Macchi, P., Donghi, D. & Sironi, A. *J. Am. Chem. Soc.* **127**, 16494–16504 (2005).
38. Gatti, C. & Lasi, D. *Faraday Discuss.* **135**, 55–78 (2007).
39. Macchi, P. & Sironi, A. *Coord. Chem. Rev.* **238**, 383–412 (2003).
40. Van der Maelen, J. F. *J. Organometallics*, **39**, 1, 132–141 (2020)
41. Low, A. A., Kunze, K. L., MacDougall, P. J. & Hall, M. B. *Inorg. Chem.* **30**, 1079–1086 (1991).
42. Macchi, P., Garlaschelli, L. & Sironi, A. *J. Am. Chem. Soc.* **124**, 14173–14184 (2002).
43. Venkataramanan, N. S., Sahara, R., Mizuseki, H. & Kawazoe, Y. *J. Phys. Chem. A* **114**, 5049–5057 (2010).
44. Al-Ibadi, M. A. M., Taha, A., Hasan, A. H. & Alkanabi, D.T. A. *Journal of Baghdad Science*, **17**, 488-493 (2020).